A Coordinated Droop Control Strategy for Overvoltage Mitigation in Active Distribution Networks

Georgios C. Kryonidis, *Student Member, IEEE,* Eleftherios O. Kontis, *Student Member, IEEE,* Andreas I. Chrysochos, *Member, IEEE,* Charis S. Demoulias, *Senior Member, IEEE,* and Grigoris K. Papagiannis, *Senior Member, IEEE,*

***Abstract*—In this paper, a centralized control strategy for low-voltage networks is proposed, aiming to coordinate the droop characteristics of the distributed renewable energy sources. The main objectives are the overvoltage mitigation and the optimal network operation in terms of maximum power injection and uniform power curtailment. The distinct features of the proposed method are the incorporation of droop-based control techniques into the conventional optimal power flow formulation and the use of the sensitivity theory as a means to significantly decrease the computational burden. The validity of the developed method is justified using a genetic algorithm, while extensive comparisons with conventional centralized and decentralized control strategies indicate its superior performance in the operation of low-voltage networks.**

***Index Terms*—Active power curtailment, droop control, OPF, sensitivity theory, voltage regulation.**

I. Introduction

OVER the last decade, policies for the promotion of distributed renewable energy sources (DRESs) have been adopted in national and international level to improve grid flexibility, sustainability, and efficiency [1], [2]. As a result, the number of DRES installations connected to low-voltage (LV) and medium-voltage (MV) distribution grids has been increased rapidly, enabling the transition from passive towards to active distribution networks [3]. However, this substantial change posed a series of emerging technical challenges, concerning the reliable and secure network operation [4]. To address these issues, increased monitoring and control is necessary, a goal which can be achieved in the emerging smart grids [5]. By exploiting the new, extensive ICT capabilities of the smart grids, a higher DRES penetration as well as an increased control of the network can be achieved.

Focusing on LV networks, the voltage rise is considered as the most essential problem that distribution system operators (DSOs) have to address [6]. This happens due to the reverse power flow caused by the active power injection of the installed DRESs in conjunction with the inherent resistive nature of LV grids. In the literature, several approaches have been proposed to tackle this issue. Among them, grid reinforcement is considered as a straightforward but also expensive solution for DSOs [7]. The use of the on-load tap changers (OLTC) in the MV/LV transformer for voltage regulation can be considered as an alternative, but barely as an effective approach, due to its limited operational range [8]. In addition, high investment costs are required to replace the existing transformers with new ones equipped with OLTCs. One of the most promising approaches is the reactive power control of the DRESs, which is extensively used in MV networks since there is a strong coupling between grid voltage and reactive power [9]–[11]. However, the reactive power control is less effective in LV networks, increasing also network losses, due to the relatively high R/X ratio of the hosting lines.

Active power curtailment (APC) techniques are considered as the most efficient voltage regulation method in LV networks [12]–[15]. Generally, the APC techniques can be classified into three main categories, namely the decentralized, the distributed, and the centralized control.

Droop control of the injected active power with respect to the voltage at the point of common coupling (PCC) is considered as the most well-established decentralized method [16]–[18]. However, a number of issues may arise, which are mainly related with the optimal operation of the network. Among them, the non-uniform active power curtailment can be considered as the most significant drawback of this method. Indeed, prosumers located at the distant nodes of radial LV feeders suffer from higher power curtailment, resulting in significant loss of revenues compared to those at the beginning of the LV feeders [19].

To overcome the drawbacks of the decentralized control schemes, a number of distributed implementations have been developed [20]. In these methods, the installed DRESs communicate with each other through ICT infrastructure, aiming to achieve optimal set points. Nevertheless, all these implementations generally present degraded performance, since equilibrium points are hard to be established and excessive oscillations may be observed.

On the other hand, the main feature of the centralized control strategies is the overall management of the network following a top-down approach, by optimally dispatching DRESs

Manuscript received July 1, 2016; revised November 4, 2016 and March 17, 2017.

The authors are with the School of Electrical and Computer Engineering, Aristotle University of Thessaloniki, Thessaloniki GR 54124, Greece (e-mail: kryonidi@ece.auth.gr; kontislefteris@gmail.com; anchryso@auth.gr; chdimoul@auth.gr; grigoris@eng.auth.gr).

This work is supported by the EC-FP7 project "INCREASE" with Grant agreement: 608998. Website: http://www.project-increase.eu/.

The work of G. C. Kryonidis is supported by the Research Committee of Aristotle University of Thessaloniki via a merit scholarship between 2016 and 2017.

Citation Information: DOI: 10.1109/TSG.2017.2685686

to satisfy specific objectives [21], [22]. This is mainly attained by solving non-linear mathematical equations based on short-term load and generation forecasts, as described by the optimal power flow (OPF) theory [23]. Generally, the main drawback of these techniques lies in the excessive execution times and the sub-optimal solutions that may occur due to the inherent network non-linearities. More sophisticated techniques have been recently proposed to address the sub-optimality issues of the OPF method [24]–[26]. However, similarly to the conventional OPF techniques, these approaches cannot effectively address various reliability and security issues, which may occur in cases of generation and/or consumption forecast errors or communication failures between the central controller and the DRESs.

In this paper, a centralized droop control strategy is proposed to address the above-mentioned issues. The main objective of the proposed method is to optimize the network operation by centrally coordinating the droop characteristics of the installed DRESs. The distinct features are the incorporation of the droop control mechanism into the OPF formulation and the use of the sensitivity theory. The droop control mitigates efficiently potential overvoltages and ensures the reliable and secure network operation, even in cases of forecast errors or communication failures. On the other hand, the sensitivity matrix is introduced to linearize the network operation and significantly reduce the computational burden.

Following this introduction, the remaining of the paper is organized as follows: In Section II, the theoretical background of the OPF method is discussed. The mathematical formulation and the actual implementation of the proposed control strategy are thoroughly presented in Section III. Section IV describes the system under study, while the numerical validation of the proposed strategy is presented in Section V. The performance of the developed control scheme is compared with conventional centralized and decentralized control strategies in Section VI, while in Section VII, its effectiveness is further evaluated on the IEEE European Low Voltage Test Feeder. Finally, Section VIII summarizes the distinct advantages of the proposed method and concludes the paper.

II. Theoretical Background

In literature, OPF-based methods are used to define the optimal operation of the network. From a technical perspective, the main objectives of these methods are to minimize power losses or to maximize the injected power of the installed DRESs, satisfying also certain operational constraints, such as voltage and thermal limits.

In this paper, the minimization of the overall curtailed power is considered as the main objective of the OPF method. Moreover, the uniform power curtailment among the installed DRESs is introduced as an additional operational constraint. This constraint has been recently proposed in the literature [13], [19], [27], [28] as a potential DSO policy to overcome the unfair power curtailment problem among the DRESs equipped with $P(V)$ droop control. More specifically, since the majority of LV networks have a radial, tree-like structure [29], the DRESs located at the most distant nodes are more likely to suffer from overvoltages and thus from higher active power curtailment. Therefore, this policy aims to redistribute the curtailed power among the DRESs, providing a strong incentive for the prosumers to install new DRESs and thus leading to further DRES penetration in the existing LV networks. In this case, the OPF is formulated as a non-linear optimization problem according to (1)-(11). To facilitate the reading, the variables of the following equations are graphically represented in the typical LV network of Fig. 1.

$$\min \sum_{i \in N_{dres}} P_{curt,i} \tag{1}$$

s.t.

$$P_{curt,i} = P_{mpp,i} - P_i \quad \forall i \in N_{dres} \tag{2}$$

$$\begin{aligned} V_j^2 = \{ & V_{p(j)}^2 + 2(A_j R_j + B_j X_j) \\ & + [V_{p(j)}^4 + 4(A_j R_j + B_j X_j) V_{p(j)}^2 \\ & - 4(A_j X_j - B_j R_j)^2]^{1/2} \}/2 \quad \forall j \in N \end{aligned} \tag{3}$$

$$A_j = \sum_{k \in N_{d,j}} P_{net,k} - \sum_{k \in N_{d,n(j)}} P_{loss,k} \quad \forall j \in N \tag{4}$$

$$B_j = \sum_{k \in N_{d,j}} Q_{net,k} - \sum_{k \in N_{d,n(j)}} Q_{loss,k} \quad \forall j \in N \tag{5}$$

$$P_{loss,j} = R_j (A_j^2 + B_j^2)/V_j^2 \quad \forall j \in N \tag{6}$$

$$Q_{loss,j} = X_j (A_j^2 + B_j^2)/V_j^2 \quad \forall j \in N \tag{7}$$

$$V_{min} \leq V_j \leq V_{max} \quad \forall j \in N \tag{8}$$

$$0 \leq I_j \leq I_{max,j} \quad \forall j \in N \tag{9}$$

$$0 \leq P_{curt,i} \leq P_{mpp,i} \quad \forall i \in N_{dres} \tag{10}$$

$$\frac{P_{curt,i}}{P_{mpp,i}} = const \quad \forall i \in N_{dres} \tag{11}$$

Here, (1) denotes the objective function that minimizes the overall curtailed power. $P_{curt,i}$ is the curtailed active power of the DRES located at the i-th node, which is calculated via (2). Furthermore, $P_{mpp,i}$ stands for the maximum power point (MPP) that the DRES of the i-th node can provide at a specific time instant, while P_i is the control variable of the optimization problem, denoting the actual injected active power of the corresponding DRES.

Moreover, N is the total set of lines and network nodes omitting the slack bus, and N_{dres} denotes the set of nodes where the DRESs are connected. Network voltages are calculated using (3). In this equation, V_j and $V_{p(j)}$ are the voltage magnitudes at the j-th node and the previous adjacent one, starting from the transformer, while R_j and X_j are the resistance and reactance of the j-th line, respectively. Coefficients A_j and B_j denote the active and reactive power flowing through the j-th line, and are calculated according to (4) and (5), respectively. $P_{net,k}$ and $Q_{net,k}$ are the net injected active and reactive power of the k-th node, while $P_{loss,k}$ and $Q_{loss,k}$ are the active and reactive power losses of the k-th line, computed using (6) and (7). Note that $N_{d,j}$ is the set of nodes located downstream of the j-th node, while $n(j)$ is the set of nodes located right after the j-th node.

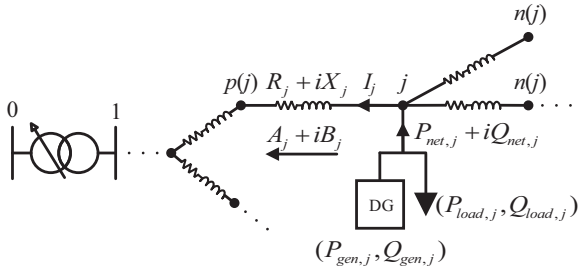

Fig. 1. Topology of a typical radial LV network.

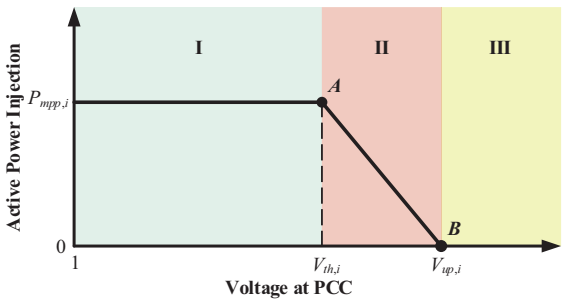

Fig. 2. A typical droop curve for the DRES connected at the i-th node.

Furthermore, V_{min} and V_{max} in (8) indicate the minimum and maximum permissible voltage limits, and are considered equal to 0.9 p.u. and 1.1 p.u., respectively, as defined by the EN 50160 Standard [30]. To avoid congestion, (9) is employed to limit the maximum current flowing through each line to the corresponding maximum ampacity. Additionally, (10) expresses an operational constraint of the DRES, representing its physical limits.

In addition, (11) is the mathematical representation of the uniform power curtailment among the installed DRESs. It is worth mentioning that different DSO policies, regarding the reallocation of APC among the DRESs, can be also adopted in the preceding formulation. For example, an alternative possible policy could assign different priorities to each DRES for its participation in the APC procedure. Such scenarios or policies can be readily incorporated as additional constraints to the problem formulation.

Considering the implementation of the OPF method in distribution networks, a centralized approach is commonly adopted. Following this, the DRESs receive set points regarding their injected active power from a central controller located at the DSO level. These set points derive from the OPF equations based on generation and consumption forecasts, and are passed through an extended communication infrastructure to the corresponding DRESs.

However, a series of technical issues may occur when these techniques are applied to extended LV distribution networks. The inherent computational complexity, which is strongly related with the network size, results in high execution times prohibiting the real-time monitoring and thus the secure operation of the network. Furthermore, it is widely accepted that these methods may suffer from sub-optimal solutions [23], [24], whereas in cases of communication loss or forecast errors, further issues can occur regarding the network operation [31], [32].

III. Proposed Control

The proposed control strategy coordinates the droop control of the injected active power with respect to the voltage at the PCC. This is succeeded by exploiting the basic formulation of the conventional OPF method, as shown in (1)-(11), and the sensitivity theory. In the next subsections, the theoretical background of droop control, the mathematical formulation, and the actual implementation of the proposed method are presented.

A. Droop Control

The main objective of the droop control is to prevent overvoltage problems by curtailing part of the total injected active power of DRESs. This strategy is quite efficient in LV networks due to their resistive nature, where a strong dependence between active power and grid voltage exists. The curtailment depends on the voltage at the PCC and is implemented by the droop curve of Fig. 2, which consists of three operation regions. In the first region, the DRES operates at the MPP power and the PCC voltage remains below the predefined voltage threshold ($V_{th,i}$). In the second region, the active power curtailment is enabled, and finally in the third one, the power injection is set to zero when the PCC voltage exceeds the maximum voltage threshold ($V_{up,i}$). The mathematical representation of the typical droop curve is expressed in (12) as a linear piece-wise function.

$$P_i = \begin{cases} P_{mpp,i} & V_i < V_{th,i} \quad (12a) \\ P_{mpp,i}\left(1 - \dfrac{V_i - V_{th,i}}{V_{up,i} - V_{th,i}}\right) & V_{th,i} \le V_i \le V_{up,i} \quad (12b) \\ 0 & V_i > V_{up,i} \quad (12c) \end{cases}$$

The incorporation of this droop control into the OPF formulation transforms the non-linear optimization problem of Section II into a mixed-integer non-linear optimization procedure, increasing considerably the numerical complexity of the solution. In this paper, this issue is addressed by simplifying the piece-wise linear function to the linear curve of (12b). The boundary limits of this linear curve are defined by the operating points *A* ($V_{th,i}$, $P_{mpp,i}$) and *B* ($V_{up,i}$, 0), as depicted in Fig. 2. Due to the fact that (12) is a continuous function and regions I and III have a zero slope, therefore providing constant power regardless the PCC voltage, the first and third regions of the droop curve can be omitted and represented as the power output defined by the operating points *A* and *B* respectively. Following this simplification, the droop control mechanism can be easily incorporated into the proposed method, avoiding the inherent complexity of the mixed-integer formulation.

B. Mathematical Formulation

The proposed control coordinates the droop characteristic of all DRESs connected to the LV network in order to minimize the total curtailed active power and succeed a uniform active power injection among the DRESs. To achieve an efficient

solution to this problem, (3)-(7) are linearized around a certain operating point by applying the sensitivity theory, while the droop control is also incorporated into the OPF formulation, using the simplified approach of the previous subsection. As a result, the optimization problem is reformulated as follows:

$$\min \sum_{i \in N_{dres}} P_{curt,i} \tag{13}$$

s.t.

$$P_{curt,i} = P_{mpp,i} - P_i \quad \forall i \in N_{dres} \tag{14}$$

$$P_i = P_{mpp,i}\left(1 - \frac{V_i - V_{th,i}}{V_{up,i} - V_{th,i}}\right) \quad \forall i \in N_{dres} \tag{15}$$

$$V_j = V_{mpp,j} - \sum_{i \in N_{dres}} c_{ji} P_{curt,i} \quad \forall j \in N \tag{16}$$

$$V_{min} \leq V_j \leq V_{max} \quad \forall j \in N \tag{17}$$

$$V_{min} \leq V_{th,i} \leq V_{max} \quad \forall i \in N_{dres} \tag{18}$$

$$V_{min} \leq V_{up,i} \leq V_{max} \quad \forall i \in N_{dres} \tag{19}$$

$$0 \leq I_j \leq I_{max,j} \quad \forall j \in N \tag{20}$$

$$0 \leq P_{curt,i} \leq P_{mpp,i} \quad \forall i \in N_{dres} \tag{21}$$

$$\frac{P_{mpp,i}}{V_{up,i} - V_{th,i}} \leq \frac{P_{rated,i}}{\beta_i} \quad \forall i \in N_{dres} \tag{22}$$

$$\frac{P_{curt,i}}{P_{mpp,i}} = const \quad \forall i \in N_{dres} \tag{23}$$

In the proposed methodology, $V_{th,i}$ and $V_{up,i}$ constitute the control variables of the optimization problem. These variables are included in (15), representing the second region of the droop control characteristic as a linear curve with variable slope. As explained previously, the two other regions of the characteristic are indirectly incorporated into the formulation, using the boundary limits of (21) in (14) and (15).

Moreover, $V_{mpp,j}$ is the voltage at j-th node when the DRESs inject their MPP. c_{ji} stands for the sensitivity matrix element that relates the voltage variation of the j-th node with respect to the total active power injection at the i-th node, whereas $P_{mpp,i}$ and $P_{rated,i}$ correspond to the MPP injection and the rated power of the DRES at the i-th node, respectively.

Generally, the sensitivity matrix is employed as a quantitative measure of the voltage magnitude and angle variations with respect to active and reactive power fluctuations. As presented in [19], it can be derived from the inverse Jacobian matrix of the network, by:

$$\begin{bmatrix} \Delta\theta \\ \Delta V \end{bmatrix} = S \begin{bmatrix} \Delta P \\ \Delta Q \end{bmatrix} = \begin{bmatrix} a & b \\ c & d \end{bmatrix} \begin{bmatrix} \Delta P \\ \Delta Q \end{bmatrix} \tag{24}$$

Since, in this paper, an APC method is adopted for the effective mitigation of overvoltages, the sub-matrix c of (24) is of main interest, as it refers to the voltage variations against the active power injections ($\Delta V/\Delta P$). This partial derivative is incorporated into the mathematical formulation of the proposed method, as shown in (16). The scope of the introduction of the sensitivity theory is twofold: First, the computational complexity is significantly reduced, resulting in relatively low execution times, and second, an efficient numerical solution can be achieved, which is not strongly dependent on the network non-linearities.

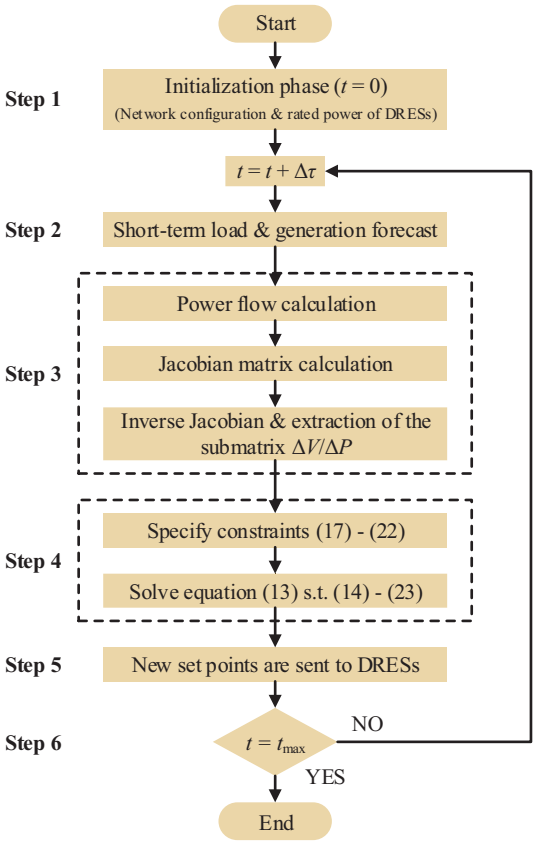

Fig. 3. Proposed algorithm.

Constraints related with the real network operation, such as the minimum and maximum permissible voltage and current limits, are imposed using (17)-(20), while operational constraints related with the physical limits of the DRESs and the uniform power curtailment are expressed with (21) and (23), respectively.

It is well accepted that for large droop coefficients, the droop control strategy may result in stability issues [33], [34]. This is caused due to the interaction among the proportional-integral (PI) controllers of the DRESs [35]. For this purpose, in this paper, the maximum acceptable slope of the droop curve is limited by employing the constraint of (22). This slope, denoted by β_i, is defined by the ratio of the rated power of the installed DRES and the minimum permissible difference between $V_{up,i}$ and $V_{th,i}$. In the general case, this slope is a user-defined parameter, which can be customized individually for each DRES based on stability analysis [34]. Nevertheless, this analysis is considered beyond the scope of this paper.

C. Actual Implementation

The implementation of the proposed centralized control algorithm is depicted in Fig. 3 by means of a flowchart. The algorithm consists of 6 main steps, as described in detail below:

Step 1: *Initialization phase*. At this Step, the data related to the network configuration as well as the rated power of

all DRESs are provided as inputs to the central controller established at the DSO level.

Step 2: *Load and generation forecast acquisition*. At each time instant, load and generation forecasts are employed for the short-term optimization of the grid. Generally, the time interval $\Delta\tau$ is DSO-defined, varying from few minutes to several hours.

Step 3: *Sensitivity matrix calculation*. A power flow calculation is first performed based on the forecasts acquired at Step 2. Then, the sub-matrix $(\Delta V/\Delta P)$ is computed by inversing the corresponding Jacobian matrix and the necessary c_{ji} coefficients of (16) are extracted.

Step 4: *Network optimization*. At this Step, the DSO imposes the operational constraints concerning the permissible limits of network voltages, line currents, and the maximum slope of the droop curve, as expressed in (17)-(22). Once these operational constraints are specified, the remaining task of the central controller focuses on the optimization of the network operation for the forthcoming time interval, by solving (13) subject to (14)-(23).

Step 5: *Dispatch of DRESs*. The new set points of $V_{th,i}$ and $V_{up,i}$ are forwarded to the corresponding DRES, as acquired from the previous Step.

Step 6: *End of control session*. At this Step, if the maximum number of time instants has been reached, the control session is completed. Otherwise, the procedure moves to Step 2.

IV. System Under Study

The performance of the proposed method is evaluated by conducting time-series simulations on a tree-like, radial LV network. The examined network is depicted in Fig. 4, consisting of 10 DRESs and 14 constant power loads. In this study, only one type of DRESs is considered, i.e. PV units. The nodes with the red color denote the location of the PV units. The rated active power of all loads and PV units, numbered according to their connection node, is presented in Table I. The power factor of the loads is considered constant and equal to 0.95 lagging for the whole simulation period, although it can have any arbitrary value. The line impedance is $0.6538+i0.0769\ \Omega$/km for the backbone of the network and $0.9393+i0.0909\ \Omega$/km for the remaining branches, whereas the corresponding lengths are listed in Table II. The MV/LV transformer has the following rating: $20/0.4$ kV, Dyn5 with nominal power of 250 kVA, short-circuit voltage of 4%, while the no-load losses and full-load losses are 330 W and 3300 W, respectively.

The simulation period of the analysis is equal to one day. Normalized typical load and generation profiles, similar to those depicted in Fig. 5, are employed. The former consists of residential and commercial load profiles, while the latter includes sunny and cloudy generation patterns. The daily load or generation profile at each node is obtained by multiplying the rated power of each load or PV unit with the corresponding normalized profile. Concerning the results presented in the next Sections, a 15-minute time interval is assumed for all examined cases, while β_i variable of (22) is considered equal to 0.01 p.u. for all DRESs.

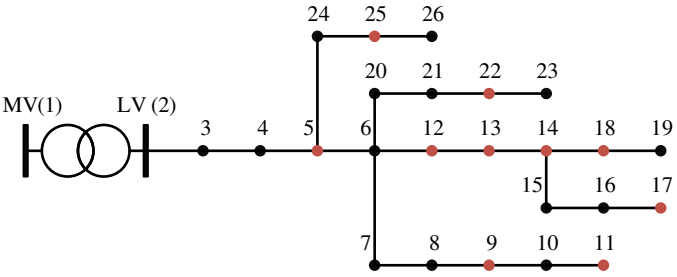

Fig. 4. LV network topology.

TABLE I
Rated Active Power Generation and Consumption

PV unit	**PV 5**	**PV 9**	**PV 11**	**PV 12**	**PV 13**
kW	15	20	15	15	15
PV unit	**PV 14**	**PV 17**	**PV 18**	**PV 22**	**PV 25**
kW	10	25	30	25	25
Load	**Load 3**	**Load 4**	**Load 6**	**Load 7**	**Load 8**
kW	5	7.5	12.5	5	7.5
Load	**Load 10**	**Load 15**	**Load 16**	**Load 19**	**Load 20**
kW	10	5	10	7.5	7.5
Load	**Load 21**	**Load 23**	**Load 24**	**Load 26**	
kW	7.5	10	2.5	2.5	

TABLE II
Line Lengths

Line	**2-3**	**3-4**	**4-5**	**5-6**	**6-7**	**7-8**
Length (m)	50	100	75	25	25	50
Line	**8-9**	**9-10**	**10-11**	**6-12**	**12-13**	**13-14**
Length (m)	25	50	75	75	40	50
Line	**14-15**	**15-16**	**16-17**	**14-18**	**18-19**	**6-20**
Length (m)	50	25	50	40	50	25
Line	**20-21**	**21-22**	**22-23**	**5-24**	**24-25**	**25-26**
Length (m)	50	75	50	50	75	50

V. Numerical Validation

The numerical performance of the proposed control strategy is investigated in this Section.

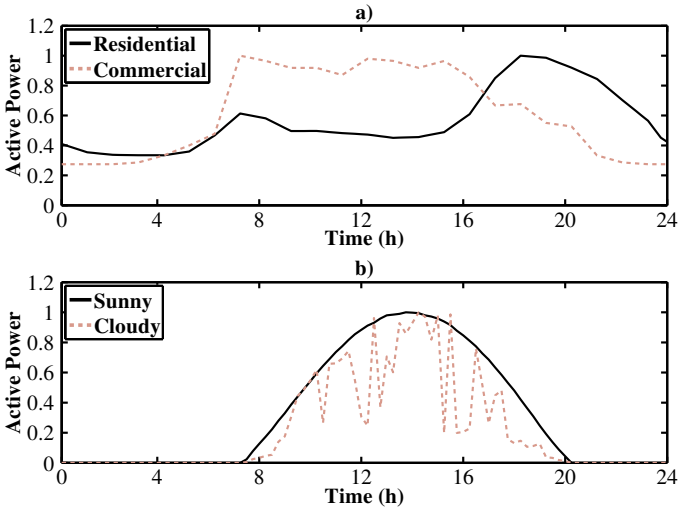

Fig. 5. Normalized active power profiles. a) Load profiles and b) generation profiles.

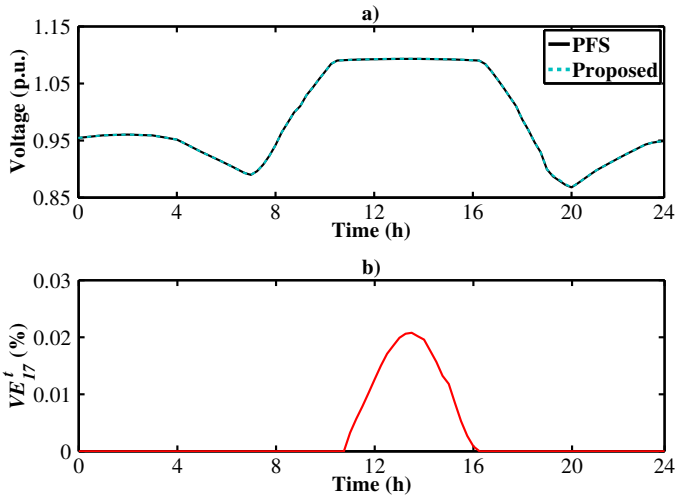

Fig. 6. Evaluation of the proposed method. a) Daily voltage profile of node 17 and b) relative percentage error.

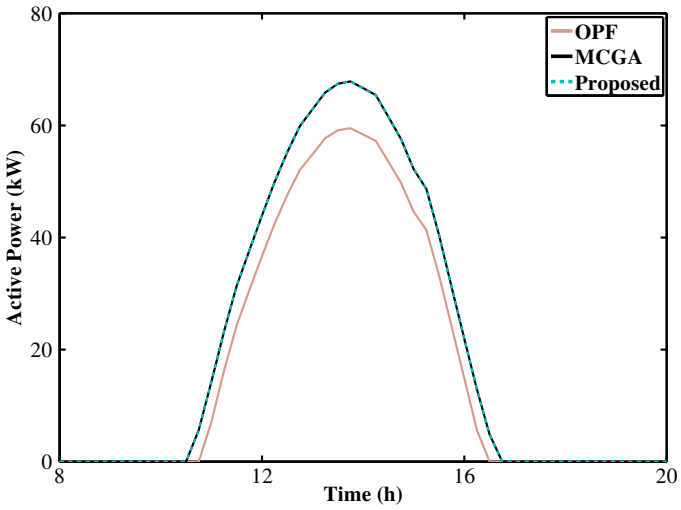

Fig. 7. Total curtailed power.

TABLE III
PERCENTAGE RELATIVE ERRORS

	Min	Max	Mean	σ
$\boldsymbol{VE_i^t}$ **(%)**	0	0.0369	0.0037	0.0014
$\boldsymbol{CE^t}$ **(%)**	0.269	1.338	0.489	0.296

A. *Effect of Linearization*

According to the proposed method, the network is linearized around a certain operating point by employing (16). Thus, it is important to investigate the impact of this assumption on the precision of the solution. For this purpose, the following procedure is adopted: The mathematical formulation of the developed method, as given by (13)-(23), is solved using the interior-point algorithm in MATLAB and the decision variables, which determine the set points ($V_{th,i}$, $V_{up,i}$) of the droop curves, are derived. Afterward, the results of the proposed method are compared with those obtained from a power flow simulation (PFS) using the full, nonlinear representation of the network. The PFS is conducted with the simulation tool developed in [36], where the set points of the droop curves are defined from the resulted decision variables calculated by the proposed method.

The numerical accuracy of the proposed control strategy is evaluated by introducing the following percentage relative errors:

$$VE_i^t(\%) = 100\frac{|V_{pfs,i}^t - V_{proposed,i}^t|}{V_{pfs,i}^t} \quad \forall i \in N \tag{25}$$

$$CE^t(\%) = 100\frac{|CP_{pfs}^t - CP_{proposed}^t|}{CP_{pfs}^t} \tag{26}$$

where $VE_i^t(\%)$ denotes the percentage relative error for the voltage magnitude of the i-th node at time instant t. On the other hand, $CE^t(\%)$ is the percentage relative error of the overall curtailed power at time instant t. Moreover, V_i^t and CP^t stand for the voltage magnitude and overall curtailed power of the DRESs, calculated for the two examined approaches, i.e. the exact PFS and the proposed method.

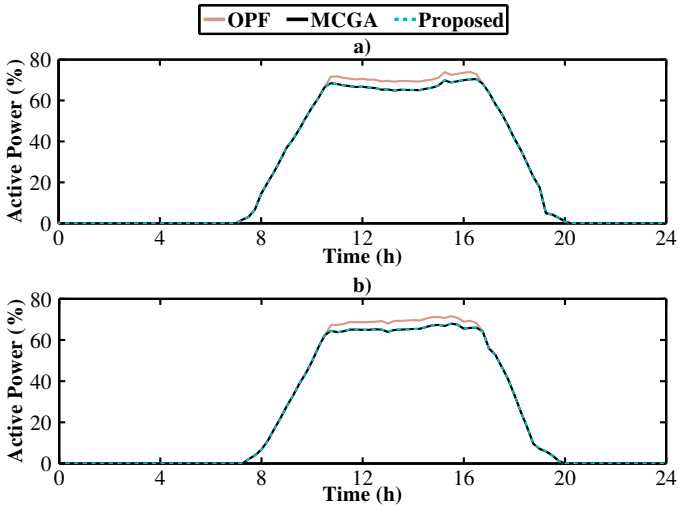

Fig. 8. Injected power. a) PV17 and b) PV25.

Simulations are conducted assuming a sunny day. The daily voltage profile of node 17 is depicted in Fig. 6. It can be shown that both the proposed and the PFS method present almost the same accuracy. In fact, only negligible percentage relative errors are observed, as depicted in Fig. 6b. To further validate the proposed control strategy, similar comparisons are conducted for all other network nodes. The minimum, maximum and average relative error, and the standard deviation (σ) are depicted in Table III. Based on the presented results, it can be concluded that the proposed linearization does not practically affect the accuracy of the solution.

B. *Numerical Performance*

As mentioned in Section V-A, (13)-(23), which formulate the proposed control scheme, are solved using the interior-point algorithm. In order to investigate the numerical performance of the developed method, (13)-(23) are also solved by employing a metaheuristic technique, i.e. the genetic algorithm (GA).

Concerning the initial conditions for the proposed method using the interior-point algorithm, network voltages for each

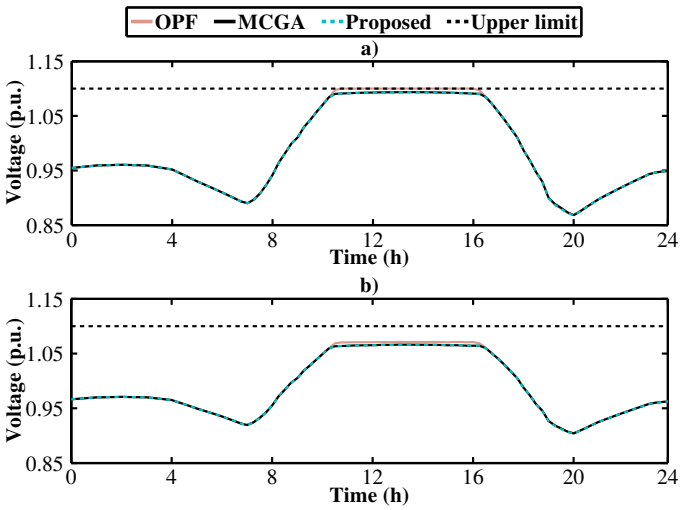

Fig. 9. Voltages at the PCC. a) PV17 and b) PV25.

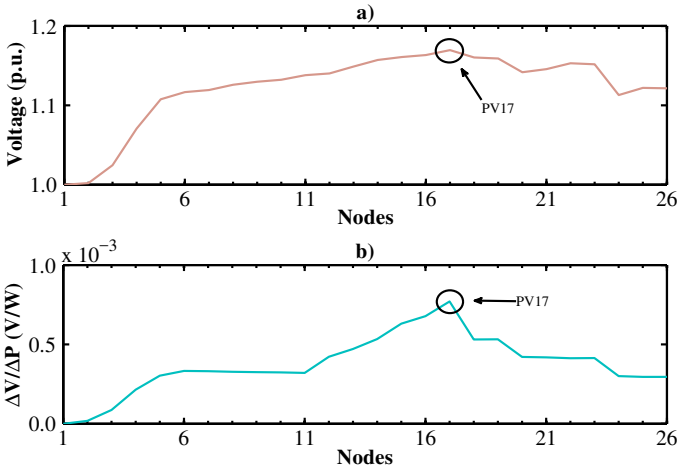

Fig. 10. Maximum generation time instant with deactivated droop control. a) Voltage profile along the network and b) elements of the sensitivity matrix related to node 17.

TABLE IV
DROOP SLOPES (W/V) FOR EACH PV UNIT

Unit	Maximum	Calculated	Unit	Maximum	Calculated
PV 5	-3750	-724.55	**PV 14**	-2500	-1450.50
PV 9	-5000	-1420.70	**PV 17**	**-6250**	**-6250**
PV 11	-3750	-1287.83	**PV 18**	-7500	-4911.30
PV 12	-3750	-1341.75	**PV 22**	-6250	-3056.88
PV 13	-3750	-1689.45	**PV 25**	-6250	-1616.63

time instant are calculated on the MPP operation of the PV units, while $V_{th,i}$ and $V_{up,i}$ are considered equal to 1.075 p.u. and 1.1 p.u., respectively. On the other hand, considering the GA, 20 distinct initial populations are randomly generated by applying the Monte-Carlo (MC) method at each time instant. The MC method is adopted in an attempt to reduce the dependence of the GA solution on the initial population and to guarantee an near-optimal solution. In each MC-based GA (MCGA) simulation, the initial population of the GA is considered equal to 1000, while the maximum number of generations is 200.

The total active power curtailment of the installed PV units for a sunny day is depicted in Fig. 7, whereas the injected active power and the voltage profiles of specific PV units are shown in Fig. 8 and Fig. 9, respectively. In these figures, the results of the proposed method are compared to the corresponding of the OPF and of the best solution, in terms of minimum curtailed power, provided by the MCGA implementation. According to the time-series simulations, the proposed technique results in an active power curtailment close to the optimal solution, as verified by the MCGA approach. This is justified by the negligible mismatch of the curtailed power between these two methods, as shown in Fig. 7. Indeed, the maximum mismatch is equal to 0.09% (60 W out of 67 kW in absolute values), indicating the robustness and high accuracy of the developed method. It is also noted that all remaining MCGA solutions practically overlap, presenting negligible differences compared to the proposed method.

Considering the proposed method, the optimality of the solution can be also verified by the qualitative analysis of the results. Particularly, the calculated slope of the droop curve for each PV unit and the corresponding maximum permissible limits are shown in Table IV for the time instant with the maximum generation. Moreover, the network node voltages, when the PV units operate at their MPP, are presented in Fig. 10a. It is evident that the maximum voltage is observed at node 17, where PV17 is installed. The elements of the sensitivity sub-matrix c, related to node 17 with the highest voltage (c_{17i}), are shown in Fig. 10b and are used to determine the contribution of each PV unit to the voltage regulation. It is clear that the PV unit located at node 17 has the greatest impact on the corresponding voltage. Therefore, to mitigate overvoltages and minimize the curtailed power in a uniform way, the curtailment of PV17 must be minimized. This can be attained by increasing the slope of the corresponding droop curve up to its maximum limit, which is indeed the actual case as verified by the results depicted in Table IV.

VI. COMPARISON WITH CONVENTIONAL CONTROL SCHEMES

In this section, the performance of the proposed control strategy from a power systems point of view is thoroughly compared with the OPF method as well as with conventional decentralized approaches.

A. Comparison with the OPF Method

The droop control of the PV units is not incorporated into the mathematical formulation of the OPF method and thus the

TABLE V
AVERAGE EXECUTION TIME (S) FOR DIFFERENT NETWORK SIZES

Number of Nodes	OPF	Proposed	Difference (%)
5	1.57	0.08	-94.90
10	2.83	0.11	-96.11
15	4.29	0.50	-88.34
20	4.41	0.84	-80.95
25	15.28	1.10	-92.80

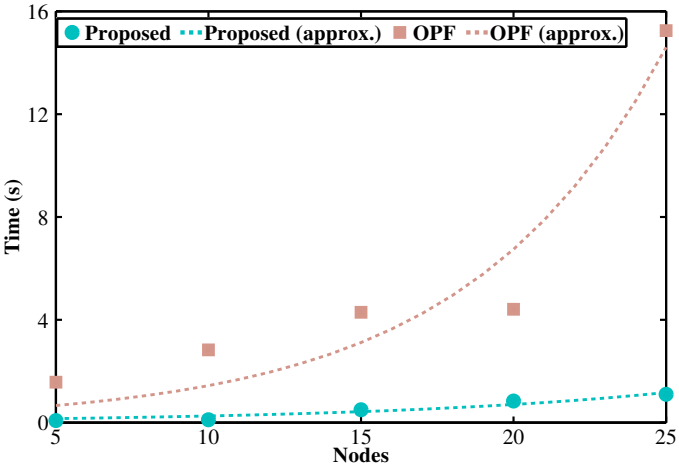

Fig. 11. Average execution times for different network sizes.

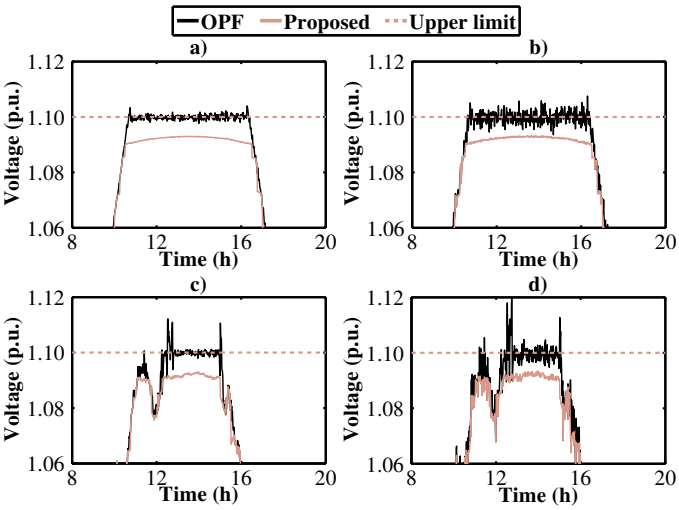

Fig. 12. Voltage profile of PV17. a) Sunny (5% forecast error), b) sunny (15% forecast error), c) cloudy (5% forecast error), and d) cloudy (15% forecast error).

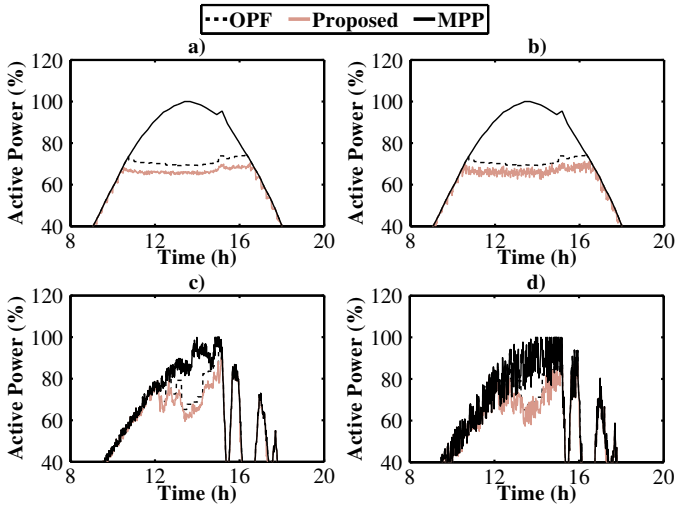

Fig. 13. Power Injection of PV17. a) Sunny (5% forecast error), b) sunny (15% forecast error), c) cloudy (5% forecast error), and d) cloudy (15% forecast error).

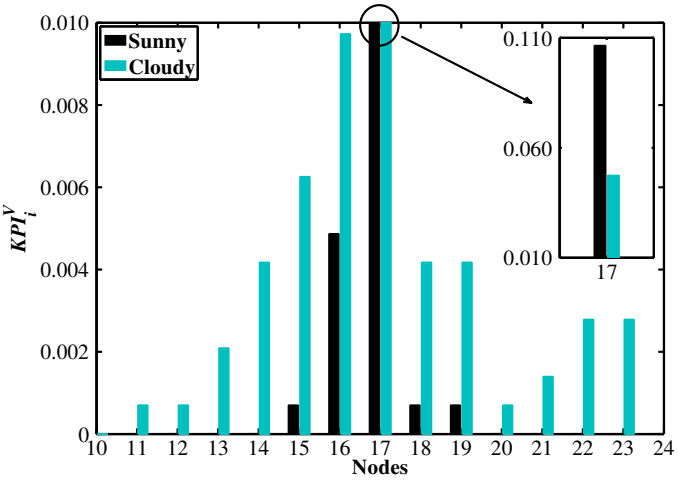

Fig. 14. Calculated KPI_i^V of the OPF method for a sunny and cloudy day.

network voltage operational limits can be fully exploited. This can be also verified in Fig. 9. Therefore, the injected power can be increased until reaching the maximum upper voltage limit, resulting in a higher power injection compared to the proposed method, as illustrated in Fig. 7 and Fig. 8.

Although the OPF method provides a higher power injection, excessive execution times may occur in extended LV distribution grids, due to the increased network complexity. To demonstrate this effect, Table V is introduced, where the average execution time during the generation period is presented for 5 different network topologies, which constitute subsets of the main grid depicted in Fig. 4. The first topology includes the first 5 LV nodes, the second one consists of the first 10 nodes, and finally the fifth coincides with the examined grid. According to Table V, it is evident that the execution time for the OPF method is highly related with the network size, presenting an exponential growth, as shown in Fig. 11. Generally, LV networks consist of hundreds of nodes, thus the implementation of the OPF may become prohibitive, especially in cases with small time interval ($\Delta\tau$). On the other hand, it is clear that the proposed method reduces the overall computational burden, resulting in significantly smaller execution times.

The implementation of both the proposed control strategy and conventional OPF method are based on short-term load and generation forecasts. However, it is widely accepted that in real field conditions forecasts errors may occur [31]. Scope of the following analysis is to verify the robustness of the developed control scheme over the OPF method in such cases. For this purpose, time-series simulations for a sunny and cloudy day are conducted, assuming 15-minute forecasts. The injected power of the PV units in both methods are calculated based on the short-term load and generation forecasts of Fig. 5. The generation and consumption profiles of Fig. 5 are then randomly distorted to emulate forecast errors. For the OPF case, if the actual available power is less than the calculated value, based on the forecast, the DRES injects the actual available power. Otherwise, the calculated power by the OPF method is injected. Since in this process the actual load conditions are not taken into account, overvoltage violations may occur due to consumption forecast errors. Numerical

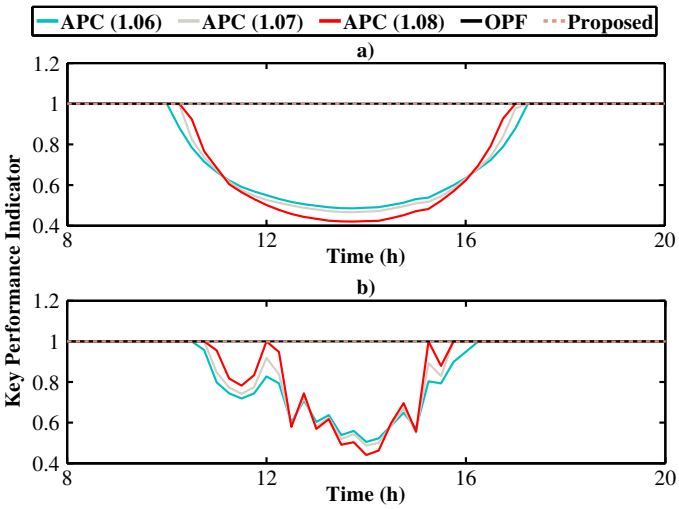

Fig. 15. Key performance indicator profile. a) Sunny day, b) cloudy day.

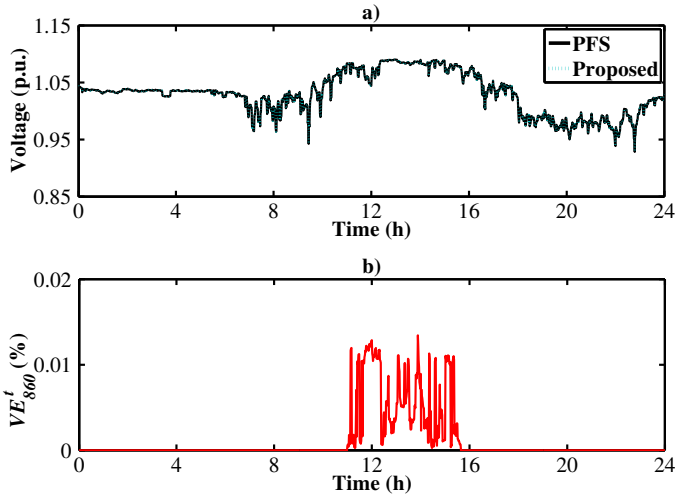

Fig. 16. Evaluation of the proposed method. a) Daily voltage profile of node 860 and b) relative percentage error.

results are presented in Fig. 12 and Fig. 13, where the voltage profile of node 17 and the active power injection of the corresponding PV unit are depicted, respectively.

In all examined scenarios, the OPF method fails to preserve the network voltages below the maximum permissible limit of 1.1 p.u., while excessive voltage fluctuations are also observed. On the other hand, the proposed method ensures the network operation within the permissible limits, mitigating considerably the voltage fluctuations. More specifically, the OPF control scheme defines specific injection set points for each 15-minute forecast interval. These set points remain constant during the considered interval. Therefore, in case of divergences from the forecasted values, overvoltages are likely to occur as verified in Fig. 12.

The incorporation of the droop control mechanism into the PV units addresses effectively the voltage fluctuation issue by controlling the active power injections. However, it is worth noticing that this results in an increased number of power injection fluctuations. This inherent characteristic of the proposed control strategy is considered of great importance, since it ensures the smooth and safe network operation, either in considerable forecast errors as presented in the previous analysis or in cases where communication failures between the central controller and the PV units occur.

To further demonstrate the advantages of the developed method in terms of avoiding overvoltage violations, the following key performance indicator (KPI) is proposed:

$$KPI_i^V = \frac{1}{T}\sum_{t\in T} a_i^t \Delta\tau \quad \forall i \in N \tag{27}$$

where KPI_i^V denotes the corresponding KPI factor of the i-th node, whereas T is the total simulation period and $\Delta\tau$ is the time interval. Finally, a_i^t is an index of the i-th node at time instant t that takes two discrete values. In case of overvoltage, a_i^t is considered equal to 1, otherwise it is set to 0.

The KPI_i^V factor of the OPF method presented in Fig. 14, indicates that overvoltage violations occur for several nodes of the network during the day. On the other hand, the corresponding KPI_i^V factors for the proposed method are always equal to zero, since this method guarantees the network operation within the permissible voltage limits.

B. Comparison with Conventional Droop Control

Furthermore, the performance of the developed control is compared with the conventional PV droop control strategy [17], by means of achieving uniform active power curtailment among the installed PV units. To evaluate the uniformity of power curtailment, the following KPI is introduced:

$$KPI_t^{inj} = \frac{\min(\boldsymbol{P}_{inj,t}(\%))}{\max(\boldsymbol{P}_{inj,t}(\%))} \quad \forall t \in T \tag{28}$$

where $\boldsymbol{P}_{inj,t}$ denotes the vector of the normalized injected power of the PV units to the corresponding MPP at time instant t. A KPI factor close to 1 indicates an almost uniform power curtailment among the PV units. In Fig. 15, the KPIs for three distinct implementations of the conventional PV droop control strategy as well as for the OPF method are compared with the proposed approach. The three discrete implementations of the droop control refer to different values of the V_{th}, namely 1.06, 1.07, and 1.08 p.u. It is evident that the conventional control scheme cannot ensure a uniform power curtailment among the PV units. On the contrary, the KPIs for the OPF method and the proposed control strategy are always equal to 1, indicating the uniformity of the power curtailment.

VII. Further Investigation on the Effect of Linearization

In this Section, the effect of linearization on the accuracy of the proposed method is further evaluated on the IEEE European Low Voltage Test Feeder [37]. This benchmark network is a typical European three-phase LV radial feeder with a nominal voltage of 416 V, consisting of 906 buses and 55 residential loads. Additionally, 15 PV units are considered. The nominal power and connection node of these PV units are presented in Table VI.

Time-series simulations are conducted for a sunny day using the generation profiles of Fig. 5b. Concerning the time-varying

TABLE VI
RATED ACTIVE POWER GENERATION AND CONSUMPTION

PV unit	**PV 1**	**PV 2**	**PV 3**	**PV 4**	**PV 5**
Node	74	83	249	289	327
kW	2	4	3	3	4
PV unit	**PV 6**	**PV 7**	**PV 8**	**PV 9**	**PV 10**
Node	337	458	611	629	682
kW	1	4	4	3	3
PV	**PV 11**	**PV 12**	**PV 13**	**PV 14**	**PV 15**
Node	702	813	817	835	860
kW	3	3	2	1	3

TABLE VII
PERCENTAGE RELATIVE ERRORS

	Min	**Max**	**Mean**	σ
$\boldsymbol{VE_i^t}$ **(%)**	0	0.0178	0.005	0.003
$\boldsymbol{CE^t}$ **(%)**	0.094	2.323	1.540	0.326

behavior of loads, the typical consumption profiles of [37] are used. The results of the proposed methodology are compared with the corresponding acquired from a power flow simulation (PFS) using the full, nonlinear network model, as discussed in Section V-A. Voltage profiles for an indicative network node and the corresponding VE_{860} (%) are depicted in Fig. 16. Furthermore, the statistical evaluation of VE_i^t and CE^t for all PV nodes is presented in Table VII. The presented results verify that the proposed control strategy can be also readily applied to extended LV, radial, distribution grids without loss of accuracy due to the adopted linearization of the network operation.

VIII. DISCUSSION AND CONCLUSIONS

In this paper, a smart coordinated approach for overvoltage mitigation in active LV distribution grids is proposed. The distinct feature of the developed control strategy is the coordinated operation of the droop characteristics among the installed DRESs of the network, in order to minimize the active power curtailment of the installed DRESs in a uniform way. For this purpose, the basic formulation of the OPF method is modified by exploiting the sensitivity theory and incorporating the droop control scheme.

The proposed control strategy aims to address the following issues, derived from the OPF implementation and the droop control method:

- Computational complexity. Generally, the extended size of LV distribution grids introduces an increased computational burden for the conventional OPF method. This is mainly related to the inherent non-linearities of the network. To overcome this issue, the sensitivity matrix is employed to linearize the network operation. This enhancement results in the significant reduction of the execution times, as verified in Section VI-A. Furthermore, simulation results of Section V-A, where the proposed methodology is compared with the full, nonlinear representation of the network, indicate that this linearization around a certain operating point does not practically affect the solution accuracy of the optimization problem. This remark is also verified in Section VII by conducting time-series simulations on the large, complex IEEE European Low Voltage Test Feeder.
- Sub-optimal solutions. Another issue is the sub-optimal solutions that may be introduced by the network non-linearities during the optimization process. The use of the sensitivity matrix in the proposed method simplifies the optimization problem and thus these sub-optimal solutions are prevented. This is validated in a quantitative as well as qualitative way by the simulation results of Section V-B. More specifically, the developed method is compared with a MC-based GA implementation and in all cases a good agreement among the corresponding results is observed. Therefore, this can be considered as a strong indicator that the proposed method reaches a near-optimal solution.
- Safe network operation. OPF methods are based on load and generation forecasts to calculate the injection set points of the DRESs. Nevertheless, in cases of erroneous set points, caused by either forecast errors or communication failure, overvoltages are likely to occur, affecting the secure network operation. This is thoroughly investigated in Section VI-A, where a key performance indicator (KPI_i^V) is proposed to assess the overvoltage mitigation capability of both the proposed and OPF methods. The corresponding results indicate that the OPF method cannot ensure the secure network operation. On the other hand, this problem is effectively addressed by incorporating the droop control into the proposed strategy.
- Optimized operation. The conventional decentralized droop control techniques cannot ensure the optimized network operation by means of maximizing the overall injected active power and achieving uniform active power curtailment. The proposed control centrally coordinates the droop characteristics of the installed DRESs, and thus guarantees the maximum power injection in a uniform way among the DRESs.

Based on the above-mentioned advantages, the proposed control scheme constitutes a valuable tool for both DSOs and prosumers, towards the proliferation of the DRESs in the existing LV networks, facilitating the transition to the Smart Grid concept.

REFERENCES

[1] *On the promotion of the use of energy from renewable sources and amending and subsequently repealing directives 2001/77/EC and 2003/20/EC*, Directive 2009/28/EC, European Parliament and Council, Brussels, Belgium, 2009, pp. 16-62.

[2] M. Madrigal, M. Bhatia, G. Elizondo, A. Sarkar, and M. Kojima, "Twin peaks: Surmounting the global challenges of energy for all and greener, more efficient electricity services," *IEEE Power Energy Mag.*, vol. 10, no. 3, pp. 20–29, May 2012.

[3] L. F. Ochoa, C. J. Dent, and G. P. Harrison, "Distribution network capacity assessment: Variable dg and active networks," *IEEE Trans. Power Syst.*, vol. 25, no. 1, pp. 87–95, Feb 2010.

[4] R. A. Walling, R. Saint, R. C. Dugan, J. Burke, and L. A. Kojovic, "Summary of distributed resources impact on power delivery systems," *IEEE Trans. Power Del.*, vol. 23, no. 3, pp. 1636–1644, July 2008.

[5] G. T. Heydt, "The next generation of power distribution systems," *IEEE Trans. Smart Grid*, vol. 1, no. 3, pp. 225–235, Dec 2010.

[6] C. L. Masters, "Voltage rise: the big issue when connecting embedded generation to long 11 kv overhead lines," *Power Eng. J.*, vol. 16, no. 1, pp. 5–12, Feb 2002.

[7] A. Kulmala, S. Repo, and P. Jrventausta, "Coordinated voltage control in distribution networks including several distributed energy resources," *IEEE Trans. Smart Grid*, vol. 5, no. 4, pp. 2010–2020, July 2014.

[8] H. E. Farag, E. F. El-Saadany, and R. Seethapathy, "A two ways communication-based distributed control for voltage regulation in smart distribution feeders," *IEEE Trans. Smart Grid*, vol. 3, no. 1, pp. 271–281, March 2012.

[9] F. A. Viawan and D. Karlsson, "Voltage and reactive power control in systems with synchronous machine-based distributed generation," *IEEE Trans. Power Del.*, vol. 23, no. 2, pp. 1079–1087, April 2008.

[10] P. M. S. Carvalho, P. F. Correia, and L. A. F. M. Ferreira, "Distributed reactive power generation control for voltage rise mitigation in distribution networks," *IEEE Trans. Power Syst.*, vol. 23, no. 2, pp. 766–772, May 2008.

[11] G. C. Kryonidis, C. S. Demoulias, and G. K. Papagiannis, "A nearly decentralized voltage regulation algorithm for loss minimization in radial mv networks with high dg penetration," *IEEE Trans. Sustain. Energy*, vol. PP, no. 99, pp. 1–1, 2016.

[12] S. Conti, A. Greco, N. Messina, and S. Raiti, "Local voltage regulation in lv distribution networks with pv distributed generation," in *International Symposium on Power Electronics, Electrical Drives, Automation and Motion, 2006. SPEEDAM 2006.*, May 2006, pp. 519–524.

[13] R. Tonkoski and L. A. C. Lopes, "Impact of active power curtailment on overvoltage prevention and energy production of pv inverters connected to low voltage residential feeders," *Renewable Energy*, vol. 36, no. 12, pp. 3566–3574, 2011.

[14] ——, "Voltage regulation in radial distribution feeders with high penetration of photovoltaic," in *Energy 2030 Conference, 2008. ENERGY 2008. IEEE*, Nov 2008, pp. 1–7.

[15] S. Weckx, C. Gonzalez, and J. Driesen, "Combined central and local active and reactive power control of pv inverters," *IEEE Transactions on Sustainable Energy*, vol. 5, no. 3, pp. 776–784, July 2014.

[16] K. D. Brabandere, A. Woyte, R. Belmans, and J. Nijs, "Prevention of inverter voltage tripping in high density pv grids," in *19th EU-PVSEC, 2004 Paris, France*, 2004, pp. 1–6.

[17] T. L. Vandoorn, J. D. Kooning, B. Meersman, and L. Vandevelde, "Voltage-based droop control of renewables to avoid on/off oscillations caused by overvoltages," *IEEE Trans. Power Del.*, vol. 28, no. 2, pp. 845–854, April 2013.

[18] T. L. Vandoorn, B. Meersman, J. D. M. D. Kooning, and L. Vandevelde, "Transition from islanded to grid-connected mode of microgrids with voltage-based droop control," *IEEE Trans. Power Syst.*, vol. 28, no. 3, pp. 2545–2553, Aug 2013.

[19] R. Tonkoski, L. A. C. Lopes, and T. H. M. El-Fouly, "Coordinated active power curtailment of grid connected pv inverters for overvoltage prevention," *IEEE Trans. Sustain. Energy*, vol. 2, no. 2, pp. 139–147, April 2011.

[20] A. Vaccaro, G. Velotto, and A. F. Zobaa, "A decentralized and cooperative architecture for optimal voltage regulation in smart grids," *IEEE Trans. Ind. Electron.*, vol. 58, no. 10, pp. 4593–4602, Oct 2011.

[21] E. DallAnese, S. V. Dhople, and G. B. Giannakis, "Optimal dispatch of photovoltaic inverters in residential distribution systems," *IEEE Trans. Sustain. Energy*, vol. 5, no. 2, pp. 487–497, April 2014.

[22] Z. Wang, H. Chen, J. Wang, and M. Begovic, "Inverter-less hybrid voltage/var control for distribution circuits with photovoltaic generators," *IEEE Trans. Smart Grid*, vol. 5, no. 6, pp. 2718–2728, Nov 2014.

[23] H. Ahmadi and J. R. Marti, "Distribution system optimization based on a linear power-flow formulation," *IEEE Trans. Power Del.*, vol. 30, no. 1, pp. 25–33, Feb 2015.

[24] L. Gan, N. Li, U. Topcu, and S. H. Low, "Exact convex relaxation of optimal power flow in radial networks," *IEEE Trans. Autom. Control*, vol. 60, no. 1, pp. 72–87, Jan 2015.

[25] S. H. Low, "Convex relaxation of optimal power flow – Part I: Formulations and equivalence," *IEEE Trans. Control Netw. Syst.*, vol. 1, no. 1, pp. 15–27, March 2014.

[26] ——, "Convex relaxation of optimal power flow – Part II: Exactness," *IEEE Trans. Control Netw. Syst.*, vol. 1, no. 2, pp. 177–189, June 2014.

[27] M. M. V. M. Ali, P. H. Nguyen, W. L. Kling, A. I. Chrysochos, T. A. Papadopoulos, and G. K. Papagiannis, "Fair power curtailment of distributed renewable energy sources to mitigate overvoltages in low-voltage networks," in *PowerTech, 2015 IEEE Eindhoven*, June 2015, pp. 1–5.

[28] S. Alyami, Y. Wang, C. Wang, J. Zhao, and B. Zhao, "Adaptive real power capping method for fair overvoltage regulation of distribution networks with high penetration of pv systems," *IEEE Trans. Smart Grid*, vol. 5, no. 6, pp. 2729–2738, Nov 2014.

[29] A. Zidan and E. F. El-Saadany, "A cooperative multiagent framework for self-healing mechanisms in distribution systems," *IEEE Trans. Smart Grid*, vol. 3, no. 3, pp. 1525–1539, Sept 2012.

[30] *Voltage characteristics of electricity supplied by public distribution networks*, Standard EN 50160, 2010.

[31] D. Fay and J. V. Ringwood, "On the influence of weather forecast errors in short-term load forecasting models," *IEEE Trans. Power Syst.*, vol. 25, no. 3, pp. 1751–1758, Aug 2010.

[32] M. S. E. Moursi, H. H. Zeineldin, J. L. Kirtley, and K. Alobeidli, "A dynamic master/slave reactive power-management scheme for smart grids with distributed generation," *IEEE Trans. Power Del.*, vol. 29, no. 3, pp. 1157–1167, June 2014.

[33] S. V. Iyer, M. N. Belur, and M. C. Chandorkar, "Decentralized control of a line interactive uninterruptible power supply (ups)," in *Proceedings of the 2010 American Control Conference*, June 2010, pp. 3293–3298.

[34] V. Mariani and F. Vasca, "Stability analysis of droop controlled inverters via dynamic phasors and contraction theory," in *Control Conference (ECC), 2013 European*, July 2013, pp. 1505–1510.

[35] H. Li, F. Li, Y. Xu, D. T. Rizy, and S. Adhikari, "Autonomous and adaptive voltage control using multiple distributed energy resources," *IEEE Trans. Power Syst.*, vol. 28, no. 2, pp. 718–730, May 2013.

[36] G. C. Kryonidis, E. O. Kontis, A. I. Chrysochos, C. S. Demoulias, D. Bozalakov, B. Meersman, T. L. Vandoorn, and L. Vandevelde, "A simulation tool for extended distribution grids with controlled distributed generation," in *PowerTech, 2015 IEEE Eindhoven*, June 2015, pp. 1–6.

[37] IEEE PES. (2016, Feb.) Distribution test feeders. [Online]. Available: http://www.ewh.ieee.org/soc/pes/dsacom/testfeeders/index.html

Georgios C. Kryonidis (S'12) received the Dipl. Eng. Degree from the School of Electrical and Computer Engineering at the Aristotle University of Thessaloniki, in 2013. He is currently working toward the Ph.D. degree in the same university. His research interests include distributed generation and storage, renewable energy sources, and smart grids operation and control.

Eleftherios O. Kontis (S'15) received the Dipl. Eng. Degree from the School of Electrical and Computer Engineering at the Aristotle University of Thessaloniki, in 2013. Since 2013, he has been Ph.D. student at the same university. His research interests are in the field of power system modeling, simulation and dynamic analysis of distribution networks and smart grids.

Andreas I. Chrysochos (S'08-M'16) received the Dipl. Eng. and Ph.D. degrees from the School of Electrical and Computer Engineering at the Aristotle University of Thessaloniki, Greece, in 2009 and 2015 respectively. Since 2015, he has been a Post-Doc researcher at the same school. His special interests are power systems modeling, computation of electromagnetic transients, and PLC. He was a scholar of the Alexander S. Onassis Public Benefit Foundation (2012-2015, 2016-2017).

Charis S. Demoulias (M'96-SM'11) received the Diploma and Ph.D. degrees in electrical engineering from the Aristotle University of Thessaloniki, where he is currently Assistant Professor with the Electrical Machines Laboratory. His research interests include power electronics, harmonics, electric motion systems, and renewable energy sources.

Grigoris K. Papagiannis (S'79-M'88-SM'09) received his Dipl. Eng. Degree and the Ph.D. degree from the School of Electrical and Computer Engineering at the Aristotle University of Thessaloniki, where he is currently Professor and Director of the Power Systems Laboratory. His special interests are power systems modelling, computation of electromagnetic transients, distributed generation and power-line communications.